Eurographics Conference on Visualization (EuroVis) 2014
H. Carr, P. Rheingans, and H. Schumann
(Guest Editors)

Volume 33 (2014), Number 3

Metro Transit-Centric Visualization for City Tour Planning

Pio Claudio and Sung-Eui Yoon

Korea Advanced Institute of Science and Technology (KAIST)

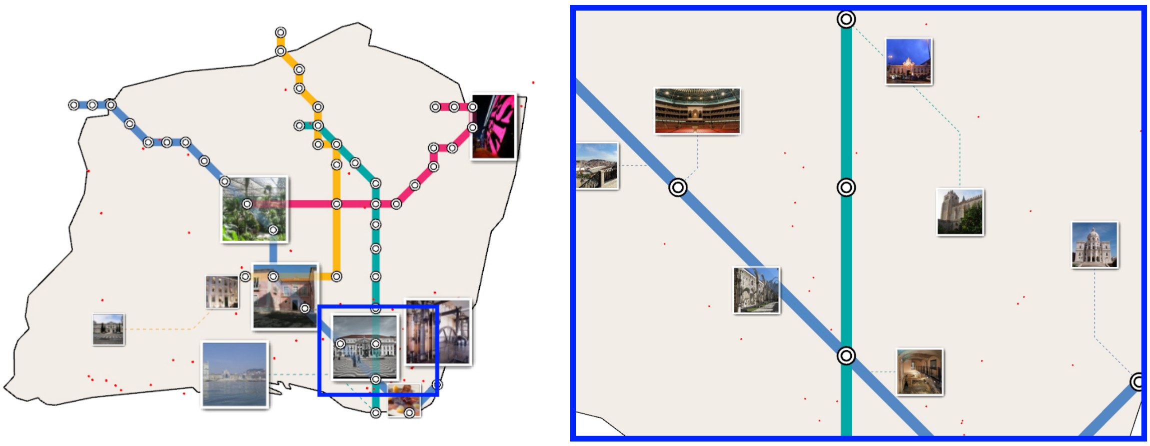

(a) Default zoom level

(b) Zoomed-in view

Figure 1: This figure shows our maps for Lisbon with different zoom levels.

Abstract

In general, city trip planning consists of two main steps: knowing Points-Of-Interest (POIs), and then planning a tour route from the current point to next preferred POIs. We mainly consider the metro for traveling around touristic cities as the main means of transportation. In this context, existing tools lack a capability to effectively visualize POIs on the metro map for trip planning. To bridge this gap, we propose an interactive framework that holistically combines presentations of POIs and a metro network. Our idea is to identify popular POIs based on visual worth computation, and to introduce POI discovery for effectively identifying POIs within reach of a metro network for users. We use octilinear layouts to highlight the metro network, and show representative POI images in the layout space visualized within a user-specified viewing window. We have implemented our working prototype showing touristic cities with a metro network. We have factored out various design guidelines that are basis for designing our method, and validated our approach with a user study surveying 70 individuals.

Categories and Subject Descriptors (according to ACM CCS): Human-centered computing [Visualization]: Visualization application domains—Geographic visualization

1. Introduction

Thanks to advances of various transportation means and increased leisure time of common people, people have more opportunities of traveling to popular tourist destinations. In traditional city trip planning, tourist destination discovery comes typically from looking at reviews or geographic map highlights (Fig. 2-(a)), and results in a list of preferred destinations. Planning a tour route among those identified tourist destinations is the next separate step, by looking at transportation maps (Fig. 2-(b)).

This decoupled approach may result in changes on the preferred destinations depending on distances and trans-

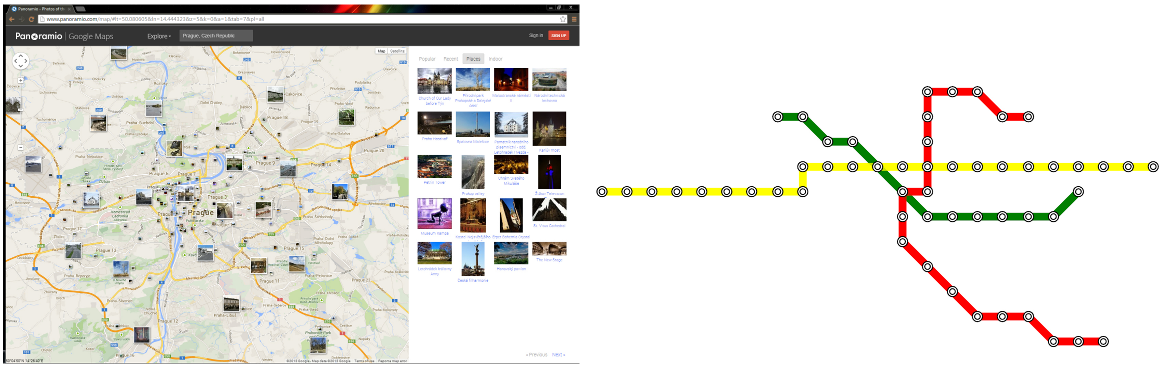

(a) Tourist destinations map (b) Schematic metro map

Figure 2: Two separate maps are commonly used for planning. (a) is a screenshot of *panoramio.com* Swapping between these two different maps can cause a mental gap for city tour planning.

portation availability. In addition, swapping from a geographic map to a transportation map creates a mental gap, as the planner tries to remember details from one map, and places and translates them into a different map. Unfortunately, prior visualization techniques for metro network [Wol07] and their labels [WTH*13] mainly focused on visualizing individual components of common city trip planning. As a result these approaches are not mainly designed for providing holistic visualization for this kind of trip planning.

Geo-tagged photo websites (Fig.2-(a)), e.g., *flickr.com* and *panoramio.com*, assist tourist destination discovery by highlighting popular photos in geographic maps. Some tour planner websites (e.g., *planner.com*) also offer popular destinations in a similar photo discovery in geographic maps. In these websites, photos are clustered and usually presented with a representative image. Display of these photos, however, are not composed by explicitly considering reachability from metro or other transportation means.

To address this problem, the metro network is commonly featured in the geographic map. Nonetheless, it can be easily buried in photos and other geographic map information such as various labels and roads. It is important to effectively show reachability from a metro map to tourist destinations during the city trip planning. An approach demonstrated in Google maps shows transit lines and an external strip of POI photos, pointing to a POI location one-at-a-time. As opposed to the approach in geo-tagged photo websites, this form belongs to *external annotation*, occupying additional precious screen estate, such that when applied to a smaller display, the screen could get easily cluttered.

Main contributions. We propose a holistic visualization technique that supports tour planners to effectively identify preferred tourist destinations and their reachability from the metro map of a chosen city (Fig. 1). To achieve our goals, our method uses the metro network as the center of planning and provides a schematic diagram of a metro map populated with representative photos. To help tour planners to effectively navigate the metro network and tourist destinations, we provide them an automated octilinear layout of the metro. In addition, we identify and highlight popular tourist areas that are also in the vicinity of metro stations.

Our method starts from both a metro network, represented with a graph, and Points-Of-Interest (POIs) provided by trip reviews websites such as *tripadvisor.com*. Each POI is associated with its name, its geographic location, genre, photos, etc. Our method identifies popular tourist areas based on kernel density estimation. We then assign high visual worths to such areas for allocating more visualization space for them (Sec. 4.1). For computing the schematic metro map in the octilinear layout, we apply a mixed integer programming approach for computing a near-optimal solution (Sec. 4.2). Once the schematic metro map is constructed, we position POIs in the map by warping geographic locations to the computed map (Sec. 4.3). We finally perform a hierarchical clustering method for computing representative images out of densely populated POIs in a small region (Sec. 4.4). Fig. 4 summarizes our method.

To validate our approach, we have conducted a user study surveying 70 individuals. We have factored out our six design guidelines and used them as a basis for designing our method. We have found that our method receives a high user satisfaction rating average of 1.097 in the range $[-2,2]$ of our Likert scale. These results demonstrate the benefits of our proposed method.

2. Related Work

We review prior methods directly related to our approach in this section.

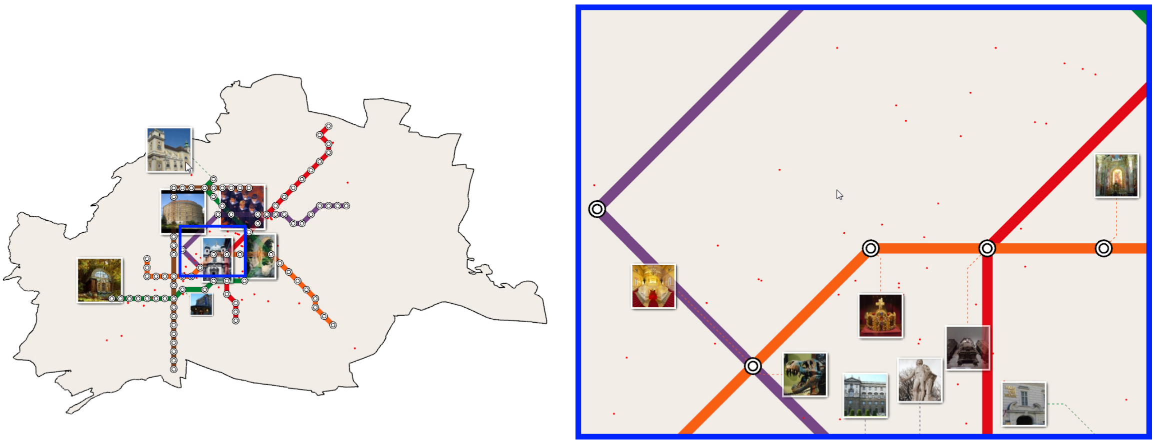

(a) Default zoom level

(b) Zoomed-in view

Figure 3: This figure shows our maps for the Vienna city with different zoom levels.

2.1. Metro Network Layout

Different approaches have been proposed for computing layouts for metro network [Wol07]. Among them, octilinear layouts using diagonal edges as well as horizontal and vertical edges have been widely adopted for visualizing metro networks.

Octilinear layouts. Automatic generation of octilinear metro map layouts has been studied in recent years. One of the initial works was of Hong et al. [HMdN06]. This approach utilizes mass spring techniques, where forces dictate relative positions to achieve octilinear layouts. Stott et. al. [SRMOW11] used a hill climbing algorithm to optimize the positions of the stations.

Nollenburg et al. [NW11] viewed the layout problem as an optimization problem, and employed a mixed integer programming (MIP) approach to find a global solution maximally satisfying design constraints. Its resulting layouts show a strict compliance to octilinearity and feature almost uniform spacing. Similar MIP techniques have been used in related layout problems [BDLN05]. Our work also utilizes MIP based optimization for computing a global solution given our design criteria.

Annotation placement. Map annotation has been well investigated, yet annotation placement in octilinear metro maps is another problem raised with automated octilinear layout generation. Wu et al. [WTLY12] used flow networks to put external annotations around the map boundaries connected by lines to the stations, while avoiding intersections with metro lines. More recently, Wu et al. [WTH*13] investigated internal annotations: placing them in the vicinity of the sources; an MIP framework proposed by Nollenburg et al. [NW11] is utilized to place annotations without overlaps, while drawing octilinear line connectors. Although the resulting internal annotations may not retain relative topology, the spacing is well distributed thanks to the additional aesthetic criteria such as alternating distribution and closed region avoidance. Nonetheless, these techniques are not designed for interactive tour planning and computing representative POIs.

Map warping. Jenny et al. [JH11] used map warping, Helmert transformation, to analyze geometric distortions of maps, and analyzed octilinear metro maps compared to its geographic counterpart. Bottger et al. [BBDZ08] used distortion by moving least squares to fit a street map in an octilinear metro map. We also apply map warping techniques for aligning POIs in the computed octilinear layout. A simple map warping method like Jenny et al. suffices for our purposes of transforming point positions. Yet more sophisticated methods exist such as Bottger et al., which can be substituted in order to perform non-overlapping transforms.

2.2. Removing Clutters

Metro maps can be populated with many associated attributes such as labels, pictures, etc. Focus+Context and computing representative images have been studied to optimize the display of these annotations.

Focus+Context. Focus and context is one of the staple techniques in the visualization community. This technique magnifies graphs and grids to focus on certain areas, while retaining the normalcy of the remaining areas as a context [KR96]. In particular, Sarkar and Brown [SB92] defined a visual worth attribute for each vertex to determine its importance in visibility. In the work of Wang et al. [WC11], as applied in metro maps, visual worth are set to be higher for edges in the selected route.

Representative images. In a map featuring hundreds of photos, a representative image is usually used to represent an area, as commonly applied in geo-tagged image websites (e.g., *flickr.com* and *panoramio.com*). An approach by Jaffe et al. [JNTD06] is to display summaries of a large collection of images by traversing a hierarchy resulting from the Hungarian hierarchical clustering method [GT08]. The representative images of a cluster are defined by their scores coming from criteria such as relevance. We find the Hungarian method useful as a hierarchical clustering method, which creates a hierarchy handily used as an LOD tree. At the same time, this method does not need a defined number of clusters as input. These techniques have not been applied to city tour planning, the main application of our method.

3. Background

In this section we go through a domain of applications addressing map switching. In particular, we view tools that explore solutions on combining metro maps with tourist/street maps.

Reilly et al. [RI04] investigated image map morphing as a tool to reconcile two different maps of the same place. One-to-one mapping points are defined to guide the image morphing process and intermediate transition images are recorded. Bottger et al. [BBDZ08] used distortion by moving least squares to fit a street map in an octilinear metro map space. Zooming-in morphs the image until it converges to the undistorted geographically accurate map. As these applications apply image distortion to the maps, resulting artifacts include curvy street lines, cross-blending. We take inspiration from these works, but we do not use image space in distorting our maps.

Our work strives to improve on creating an optimized tourist map in a single octilinear space for use in trip planning. We parallel our design principles on complementary works on trip planning such as route maps [AS01, KAB*10], which discard detailed map solutions for a clear and easy-to-read format in conveying information. Also by working in a single octilinear space through interpolation, the difficulty of adjusting between map conventions and spaces is absolved. This design can bring added usability. For example, near a tourist center, there may be many POIs and nearby metro stations. One can easily identify different routes to cover preferred POIs by taking metro transits or walking, by looking at the single octilinear layout populated with POIs.

Note that most tourist maps are still handcrafted despite automated solutions exist. Aforementioned works may not be popularly applied on their own applications yet. Nonetheless, automatically generated layouts can be used as basis by artists, as described in [WTH*13].

4. Our Approach

In this section we elaborate each part of our method. For designing these parts, we have factored out various design

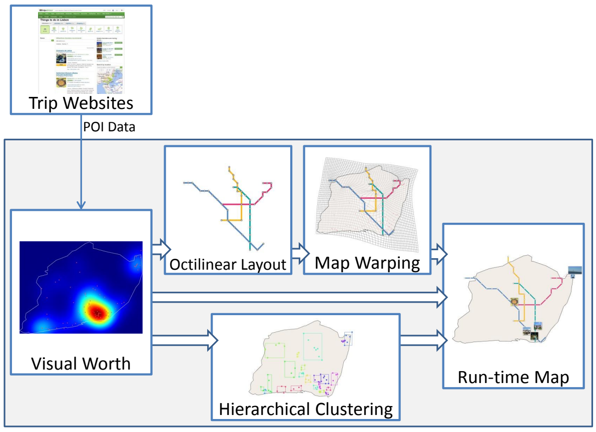

Figure 4: This figure shows the overall structure of our system.

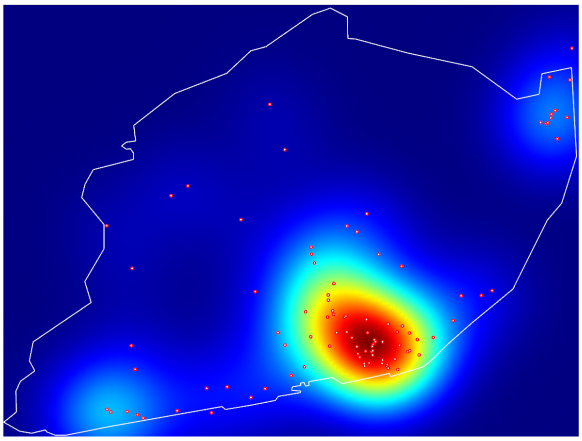

Figure 5: This figure shows a heat map of Lisbon resulting from our kernel density estimation with POIs (shown in red dots).

guidelines, which are discussed in Sec. 5.1. Based on those observations, we adapt our final design choices.

As the base information to our method, we harvest a metro network map and POIs representing interesting locations of a city from trip reviews websites like *tripadvisor.com*. In addition to harvesting basic information (e.g., name and location) for each POI, we also collect its popularity ranking among those identified POIs.

4.1. Visual Worth Computation

We aim to magnify the spaces of popular tourist areas for allocating larger visualization working spaces to them. To effectively identify such areas, we transform the problem of identifying them into a density estimation problem. Specifically, we use the variable kernel density estimation method [TS92] with the POI geographic coordinates as samples (Fig. 5).

We also utilize available ranking information, r_i, for i-th POIs and consider it in our density estimation. In particular, we emphasize highly ranked POIs. To realize our purpose, we use the POI ranking as a factor to a constant kernel bandwidth, k. In other words, lower ranked POIs are used with larger bandwidths, and thus affects visual worths on their nearby regions in low weights. We also consider the proximity, ρ_i, of POIs from the nearest metro station, since close POIs from metro stations can be also preferable for tourists.

Given a point u on a geographic map, we estimate its visual worth $vw(u)$, as the following:

$$\begin{aligned} vw(u) &= \frac{1}{n}\sum_{i=1}^{n}\frac{1}{(h_i)^2}K(POI_i,u,h_i), \qquad (1)\\ h_i &= k(w_r r_i + w_\rho \rho_i),\\ K(POI_i,u,h_i) &= \frac{1}{2\pi h_i^2}\mathrm{e}^{-\frac{d(POI_i,u)}{2h_i^2}}, \end{aligned}$$

where n is the number of samples, h_i is the variable bandwidth, K is a 2D Gaussian kernel, POI_i represents the location of i^{th} POI, and $d(POI_i,u)$ is the Euclidean distance function. w_r and w_ρ are the weights for the terms ranking r_i and proximity ρ_i.

Fig. 5 shows an example of our visual worth computation for a city. We treat high-density areas (shown in red colors) as tourist centers of the city and allocate more space for those areas in later parts of our method.

Recalling Fig. 4, the computed visual worth values directly affect later stages of our method. On one hand, we use visual worth to control edge lengths in the octilinear layout computation. On the other hand, we use visual worth to extract prominent clusters in the active cluster set.

4.2. Octilinear Layout Computation for Metro Network

We use the given metro network as the center of our visualization. To support tour planners to effectively navigate the metro network and tourist destinations, we compute an octilinear layout of the given metro network as its schematic representation. In particular, we use an MIP based optimization method for computing the octilinear layout, while minimizing costs that are measured against various octilinear layout design criteria [NW11].

For our purpose, we aim to minimize bending angles between the physical metro line and its corresponding edge in the layout, $cost_{bend}$, to preserve the original topology of the metro network, $cost_{topo}$, and to reduce the sum of edge lengths and avoid excessively long edges, $cost_{length}$. They

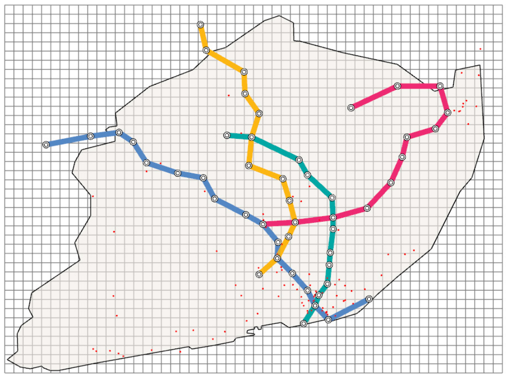

(a) Input

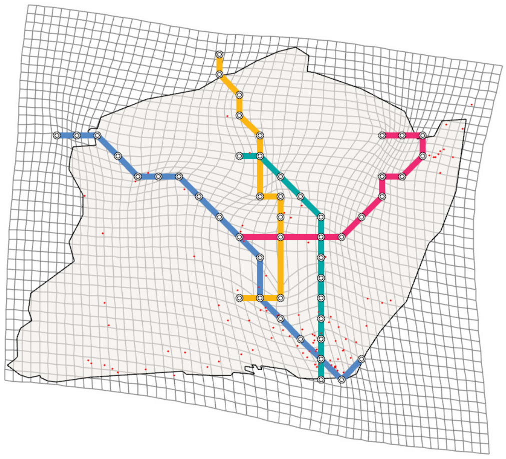

(b) Our octilinear layout w/ the uniform edge length

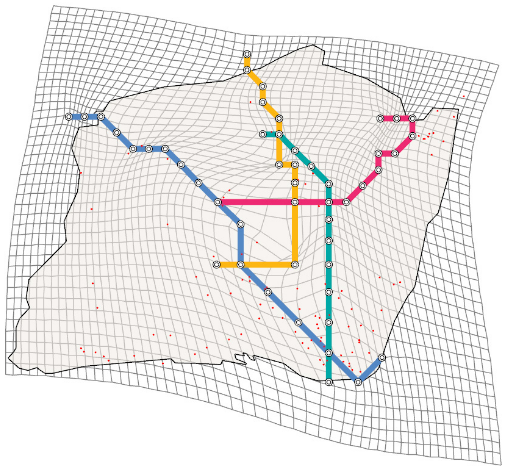

(c) Our octilinear layout w/ the variable edge length

Figure 6: (b) and (c) show computed octilinear layouts of the Lisbon metro network (a) constructed with uniform or variable edge lengths. POIs, shown in red dots, are also transformed according to the computed octilinear layout.

are defined in the following equations:

$$\begin{aligned} cost_{bend} &= \sum_{L \in \mathcal{L}} \sum_{uv,vw \in L} bd(u,v,w), \\ cost_{topo} &= \sum_{uv \in E} rpos(u,v), \\ cost_{length} &= \sum_{uv \in E} \lambda(u,v), \end{aligned} \tag{2}$$

where u, v, and w are station vertices, E is a set of metro edges in the layout. L is a geographical metro line in the set of physical metro lines, $\mathcal{L}$, and $bd(u,v,w)$ measures the bending angle between two different edges corresponding to two sub-lines, uv and vw, sampled from a geographical metro line L. $rpos(u,v)$ measures the angle difference between the edge (u,v) in the layout and its corresponding line in the metro network, and λ returns the edge length cost.

As the final cost function to the MIP optimization process, we combine these three costs with different weights; we put highest weights for $cost_{topo}$, since maintaining the relative topology of the metro network is one of the most important visualization criteria for our purpose. For all the experiments we use 1, 50, and 1 for $cost_{bend}$, $cost_{topo}$, and $cost_{length}$, respectively, as weights for the MIP optimization process.

Edges between stations are kept to have a length that is equal or higher than the minimum edge length, ℓ_{uv}. We then compute an edge length according to visual worths of two end points of the edge. The following equations define two aforementioned constraints used within our MIP optimization process for east horizontal cases:

$$x(u) - x(v) \geq \ell_{uv}, \tag{3}$$

$$\ell_{uv} = \ell_{const} \frac{vw(u) + vw(v)}{2}, \tag{4}$$

where $x(u)$ represents the x coordinate of the vertex u and ℓ_{const} is a constant factor converting from the visual worth to the edge length; we set 10 for ℓ_{const} in practice.

We also have similar equations for the other seven directions. The MIP optimization process uses constraints depending on configurations among the eight possible octilinear directions of an edge. We do not check edge overlaps, expensive constraints within our MIP optimization process, since we have found that the other used constraints combined with a small edge length, produce layouts without edge overlaps in our tested benchmarks. In a default setting, we show labels associated with metro stations, only when users click stations. This design choice is made to avoid excessive clutters. Nonetheless, we can naturally consider labels within our MIP optimization process, as mentioned in a related prior work [NW11].

Fig.6-(b) and -(c) show octilinear layouts of the Lisbon metro network that are computed by considering uniform edge lengths and ones considering the visual worth. The one constructed by considering the visual worth dedicates larger spaces for popular tourist areas.

4.3. Map Warping

In the prior section, we use the MIP optimization process to compute the octilinear layout of the given metro network. These deformed metro layouts, unfortunately, cannot be visualized together with the original coordinates of POIs. One can treat POIs as labels or other attributes associated with stations or vertices of the metro network graph, and compute their locations within the octilinear layout. We found, however, that this approach requires prohibitively excessive amount of computation time and even fails given its high time complexity, since the number of POIs can be very high (e.g., hundreds of POIs).

Instead of handling them within the MIP optimization, we adopt another step that maps POIs according to the computed octilinear layout. To map those elements into a space aligned with the computed octilinear layout, we utilize the Helmert transformation, a popular transformation method in geodesy, which is essentially a 4-parameter Euclidean transformation [JH11].

Given the Helmert transformation, we use the newly computed station positions as control points for transforming the rest of the map elements such as POI positions, city outline polygon vertices, etc. Positions of the input control points in the octilinear layout, $\bar{x_i} = \bar{x}(u)$ and $\bar{y_i} = \bar{y}(u)$, and their original positions, $x_i = x(u)$ and $y_i = y(u)$, are used to compute the four unknown parameters representing 2D translation (t_x and t_y), 1D scaling (s), and 1D rotation (θ):

$$\begin{bmatrix} \bar{x_i} \\ \bar{y_i} \end{bmatrix} = \begin{bmatrix} t_x \\ t_y \end{bmatrix} + \begin{bmatrix} s\cos\theta & -s\sin\theta \\ s\sin\theta & s\cos\theta \end{bmatrix} \begin{bmatrix} x_i \\ y_i \end{bmatrix}.$$

Given the linear system, we use a common least-squares method for computing the unknown parameters.

The next step after computing the transformation matrix for each vertex of the metro network is to construct an interpolation scheme for transforming POIs into the octilinear layout. For this purpose we adopt a multiquadric interpolation [Har90] for achieving high-quality interpolation. Specifically, we define our interpolation equation to be a quadric basis function:

$$\bar{x_i} - x_i = \sum_{j=1}^{n} \alpha_j \left((\bar{x_i} - \bar{x_j})^2 + (\bar{y_i} - \bar{y_j})^2 \right)^{-1/2}, \tag{5}$$

$$\bar{y_i} - y_i = \sum_{j=1}^{n} \beta_j \left((\bar{x_i} - \bar{x_j})^2 + (\bar{y_i} - \bar{y_j})^2 \right)^{-1/2}, \tag{6}$$

where n is the number of control points. We estimate unknown coefficients α and β based on the least-squares method.

Once we setup our interpolation equations, we then compute discrepancies, $\bar{p} - p$ and $\bar{q} - q$, for any point, (p,q), in the original map. In other words, we use the following equations to compute transformed positions $(\bar{p},\bar{q})$ given the

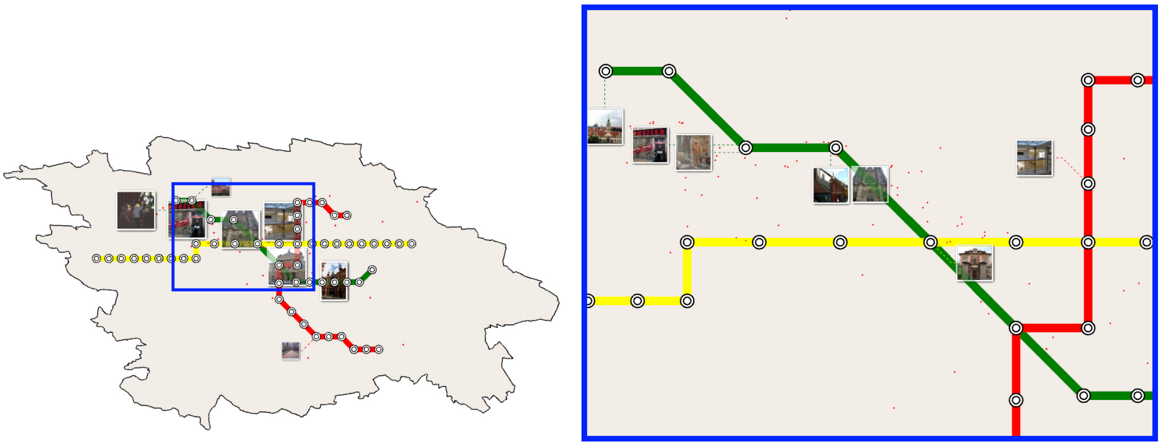

(a) Default zoom level

(b) Zoomed-in view

Figure 7: This figure shows our maps for Prague with different zoom levels.

transformed metro layout:

$$\bar{p} - p = \sum_{j=1}^{n} \alpha_j \left((\bar{p} - \bar{x_j})^2 + (\bar{q} - \bar{y_j})^2 \right)^{-1/2},$$

$$\bar{q} - q = \sum_{j=1}^{n} \beta_j \left((\bar{p} - \bar{x_j})^2 + (\bar{q} - \bar{y_j})^2 \right)^{-1/2}.$$

We visualize this transformation by showing a regular mesh and its deformed mesh in the original and octilinear layout space in Fig. 6.

4.4. Hierarchical Clustering

Displaying all POI photos can clutter the visualization result and overload users with a lot of information. Instead, we summarize the collection by computing and showing only representative images. To realize this, we use a hierarchical clustering algorithm, namely the Hungarian clustering method [GT08].

The Hungarian clustering method performs clustering based on the cycle cover problem [GT08]. In this clustering method, we start with the POI positions as inputs. We then perform the following procedures. *a*) These points are treated as initial clusters. *b*) For each cluster, we construct an edge from the cluster to the nearest cluster. We then solve a minimal cycle cover for the computed graph, resulting in a set of cycles that are treated as clustering. *c*) This is repeated for the resulting clusters in the prior step, until we cannot merge clusters anymore.

This recursive process results in a clustering tree, where each node represents a cluster, and the leaves contain individual POIs. The resulting hierarchical clustering tree is used to display a portion of the POI collection.

Runtime. At runtime, a user can zoom-in/out and translate the visualization window that shows the full or a portion of our map (Fig. 7). Given a chosen visualization window, we choose and visualize biggest POI clusters whose size is smaller than that of the window and is contained in the window. Fig. 8 shows chosen clusters given an example visualization window. To compute such clusters, defined as *active clusters*, we traverse the clustering tree from the root in the top-down manner. When we visit clusters satisfying the criteria, we treat them as active clusters and terminate the traversal from those clusters.

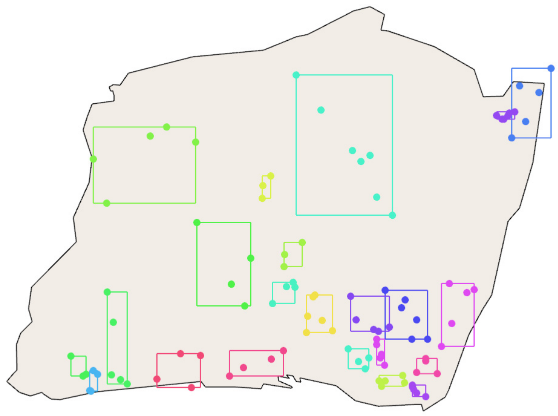

Figure 8: This figure shows our clustering result at an intermediate level.

There can be too many active clusters that cannot be visualized given the visualization window. We therefore choose top M clusters. For ordering active clusters, c_i, we compute

City	# of Stations	# of Edges	# of POIs
Lisbon	49	51	120
Prague	54	54	120
Vienna	90	96	120

Table 1: This table shows the characteristics of our tested benchmarks.

a prominence of cluster, $p(c_i)$:

$$p(c_i) = \frac{vw(c_i)}{\sum_{j=1}^{n} vw(c_j)},$$

where $vw(c_j)$ is the visual worth of the cluster c_j, which is defined as the biggest visual worth of POIs contained in the cluster. Additionally, we display the next M POIs in a smaller size to give previews of other interesting destinations. We have found that $M = 10$ works well for our purpose without cluttering the visualization. An accompanying video shows an example of using our interactive framework.

In our implementation, we only use a POI's geographic coordinate, which is assigned by tourist websites, as a single point to locate it in the map. Unfortunately, this would mean that if the point is outside the viewing window, the POI would not be displayed, even if the actual POI area is bigger. This can be addressed if a bounding box of each POI is available.

5. Results and Analysis

We have implemented our methods on a machine with a quad-core i7 3.6GHz CPU. The MIP solver used is Gurobi Optimizer (*gurobi.com*).

We have tested three benchmarks: Prague, Lisbon and Vienna data sets as shown in Fig. 7, 1, and 3, respectively. The characteristics of these three data sets are summarized in Table 1. The total preprocessing time of the visual worth computation, the MIP optimization, warping, and clustering is $0.52s$, $3.22s$ and $12.35s$ for Prague, Lisbon, and Vienna, respectively. In the visual worth computation, we set $w_r = 0.7$ and $w_\rho = 0.3$, as we have found effective based on our design factors **DF5** and **DF6**, which are discussed below. Our runtime computation that computes the most prominent, active clusters takes less than 1 ms.

5.1. Design Factors and User Study

We have designed and conducted our study to isolate design factors. Their summary is shown in Fig. 9. In order to assess our design factors, we have conducted a user study through the actual use of our interactive map prototype. We have surveyed 70 individuals: 38 females and 32 males, 16 to 35 years old. In addition to designing related questions, we have inquired about their trip planning habits. We screened

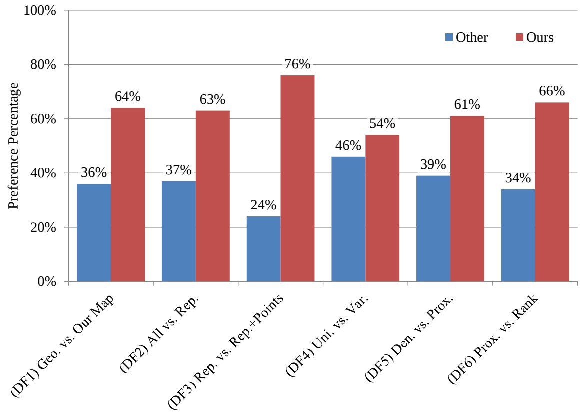

Figure 9: Design factors study results.

participants in such a way that they actually use metro-transit in their trips and are not well acquainted in the tested cities.

1. **(DF1)** Geographic vs. our map: we showed the users a geographically accurate metro map and our octilinear layout metro map, both with all the POI images. More than half of the users prefer using our map in terms of looking at a metro network and POI images. We presume that our approach might be uncomfortable to users without getting accustomed to it.
2. **(DF2)** All vs. representative photos: we showed the users our map filled with all POIs in the city and with representative POIs. We find that more users like the map with representative images. All the POIs displayed at once clutter the screen, while representative images give a clean organized look.
3. **(DF3)** Representative photos vs. representative photos+points: we showed the users our map with representative images, and with representative images and non-representative POIs displayed as small points. Users like to see what they might have been missing out, so the latter one is preferred.
4. **(DF4)** Uniform (Fig.6-(b)) vs. variable (Fig.6-(c)) edge lengths: we showed the users our map with the uniform minimum edge length and with variable minimum edge lengths. Users are slightly leaning towards variable edge lengths. As for more dense tourist areas, the variable edge factor is more valuable. This deserves further exploring in more visual perception studies.
5. **(DF5)** Density vs. proximity: we showed the users our map with a small set of POIs near the metro, and with many POIs including ones far from the metro. More users prefer to visit and see POIs nearby a metro.
6. **(DF6)** Proximity vs. ranking: we showed the users our map with a region containing far but high ranked POIs, and with another region containing near but low ranked POIs. More users prefer the high ranking tourist areas, even though it is far from the metro.

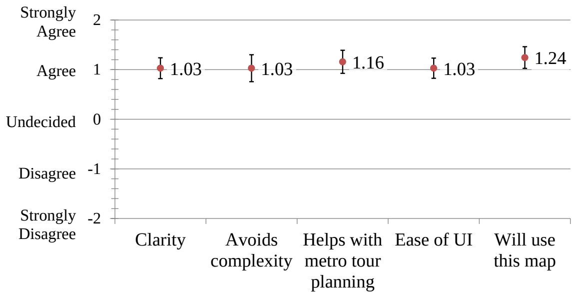

Figure 10: Average user satisfaction rating with 99% confidence intervals.

We find that significantly more participants picked ours (*p-value* < 0.05), and in particular, DF3 and DF6 trials have highly significant results (*p-value* < 0.01). However, the DF4 case has no deducible statistical significance (*p-value* $= 0.20$).

Observations from DF5 and DF6 became our basis for defining weights used in our visual worth computation (Sec. 4.1). All the other design factors have been incorporated in our method described in the prior section.

Visual Worth. Considering visual worth permits flexibility to distort the map according to multiple spatial factors. By computing visual worth with the density estimation formulation, we can naturally support proximity and ranking. It can be extended to support other factors such as POI genre, to magnify certain map areas in a different manner.

In our tested user study, many users took a while in choosing between uniform and variable edge lengths, and 54% of them selected variable edge lengths. We believe this as a result of a non-optimized parameter setting for considering proximity and ranking. Optimizing them could improve the visual worth, including the lengths of edges of the metro. Further visual cognition studies, in particular eye tracking, would greatly assist in tuning these parameters.

User Satisfaction. We have also let our users to evaluate our prototype. Fig. 10 shows the user satisfaction rating with 99% confidence intervals. Most users agreed that our map features the clarity of information and our map avoids complexity brought by overloaded information. Users find that our map would help them plan a tour-by-metro well. While our work is still a prototype, many rate our UI highly on ease of use.

Limitations. Our method has drawbacks, although it has been demonstrated to show benefits for our purpose. Our approach for visualizing annotations of POIs is *on-site*, exactly placing POIs where they are located. This approach results in unavoidable overlaps with the metro stations and edges. Our current MIP optimization is reasonably fast, but its layouts can be complex and produce edge crossings. We withhold displaying labels of stations and POIs in order to allocate more space for the metro and representative photos. Since our work provides interactive map visualization, we can conveniently show pop-up labels upon selection of a station or a POI. Our method also inherits the limitations of our employed techniques. Nollenburg's method [NW11] produces high quality globally optimized metro layouts, yet it has not been demonstrated to be applicable for complex metro networks such as Tokyo, New York or Paris.

6. Conclusion

We have proposed an interactive approach for supporting tourists to effectively identify popular tourist destinations and travel to them based on the metro network. For our holistic visualization of city trip planing, we have used visual worth computation, MIP-based octilinear layout computation combined in showing representative POIs in the layout. Additionally, we have used a hierarchical clustering method to efficiently compute representative images given a user-specified visualization window and zoom level. To validate our proposed method and factor out important design criteria that are basis for finalizing our method, we have conducted a user study, which confirmed the benefits of our method.

We have found that the proposed direction for city tour planning is promising and deserves further studies. As more geo-data is collected (location check-in, geo-tagged photos, etc.), more advanced interfaces are necessary to help tourists in planning their trips. In addition, the continued increase of smart mobile devices adaption will contribute to changing tour planning, and further trigger high demand on interactive tour guides for modern tourists [WF13]. The next logical improvement to our current system are paths to the POIs, which would require solving a different set of difficult challenges such as road simplification and layouting.

Acknowledgments

We would like to thank the anonymous reviewers, Prof. Jinwook Seo and the members of SGLab for their constructive feedbacks. This work was supported in part by NRF-2013R1A1A2058052, DAPA/ADD (UD110006MD), MEST/NRF (2013-067321), and IT R&D program of MOTIE/KEIT [10044970]. Sung-Eui Yoon is a corresponding author of the paper.

References

[AS01] AGRAWALA M., STOLTE C.: Rendering effective route maps: Improving usability through generalization. In *Proceedings of the 28th Annual Conference on Computer Graphics and Interactive Techniques* (New York, NY, USA, 2001), SIGGRAPH '01, ACM, pp. 241–249. 4

[BBDZ08] BOTTGER J., BRANDES U., DEUSSEN O., ZIEZOLD H.: Map warping for the annotation of metro maps. *IEEE Computer Graphics and Applications 28*, 5 (2008), 56–65. 3, 4

[BDLN05] BINUCCI C., DIDIMO W., LIOTTA G., NONATO M.: Orthogonal drawings of graphs with vertex and edge labels. *Computational Geometry 32*, 2 (2005), 71 – 114. 3

[GT08] GOLDBERGER J., TASSA T.: A hierarchical clustering algorithm based on the hungarian method. *Pattern Recogn. Lett. 29*, 11 (Aug. 2008), 1632–1638. 4, 7

[Har90] HARDY R.: Theory and applications of the multiquadric-biharmonic method 20 years of discovery 1968-1988. *Computers & Mathematics with Applications 19*, 8-9 (1990), 163–208. 6

[HMdN06] HONG S.-H., MERRICK D., DO NASCIMENTO H. A. D.: Automatic visualisation of metro maps. *J. Vis. Lang. Comput. 17*, 3 (June 2006), 203–224. 3

[JH11] JENNY B., HURNI L.: Cultural heritage: Studying cartographic heritage: Analysis and visualization of geometric distortions. *Comput. Graph. 35*, 2 (Apr. 2011), 402–411. 3, 6

[JNTD06] JAFFE A., NAAMAN M., TASSA T., DAVIS M.: Generating summaries and visualization for large collections of georeferenced photographs. In *Proceedings of the 8th ACM international workshop on Multimedia information retrieval* (New York, NY, USA, 2006), MIR '06, ACM, pp. 89–98. 4

[KAB*10] KOPF J., AGRAWALA M., BARGERON D., SALESIN D., COHEN M.: Automatic generation of destination maps. In *ACM SIGGRAPH Asia 2010 Papers* (New York, NY, USA, 2010), SIGGRAPH ASIA '10, ACM, pp. 158:1–158:12. 4

[KR96] KEAHEY T., ROBERTSON E.: Techniques for non-linear magnification transformations. In *Information Visualization '96, Proceedings IEEE Symposium on* (1996), pp. 38–45. 3

[NW11] NOLLENBURG M., WOLFF A.: Drawing and labeling high-quality metro maps by mixed-integer programming. *Visualization and Computer Graphics, IEEE Transactions on 17*, 5 (2011), 626–641. 3, 5, 6, 9

[RI04] REILLY D. F., INKPEN K. M.: Map morphing: Making sense of incongruent maps. In *Proceedings of the 2004 Graphics Interface Conference* (School of Computer Science, University of Waterloo, Waterloo, Ontario, Canada, 2004), GI '04, Canadian Human-Computer Communications Society, pp. 231–238. 4

[SB92] SARKAR M., BROWN M. H.: Graphical fisheye views of graphs. In *Proceedings of the SIGCHI Conference on Human Factors in Computing Systems* (New York, NY, USA, 1992), CHI '92, ACM, pp. 83–91. 3

[SRMOW11] STOTT J., RODGERS P., MARTINEZ-OVANDO J., WALKER S.: Automatic metro map layout using multicriteria optimization. *Visualization and Computer Graphics, IEEE Transactions on 17*, 1 (2011), 101–114. 3

[TS92] TERRELL G. R., SCOTT D. W.: Variable kernel density estimation. *The Annals of Statistics* (1992), 1236–1265. 5

[WC11] WANG Y.-S., CHI M.-T.: Focus+context metro maps. *Visualization and Computer Graphics, IEEE Transactions on 17*, 12 (2011), 2528–2535. 3

[WF13] WANG D., FESENMAIER D.: Transforming the travel experience: The use of smartphones for travel. In *Information and Communication Technologies in Tourism 2013*, Cantoni L., Xiang Z. P., (Eds.). Springer Berlin Heidelberg, 2013, pp. 58–69. 9

[Wol07] WOLFF A.: Drawing subway maps: A survey. *Informatik - Forschung und Entwicklung 22*, 1 (2007), 23–44. 2, 3

[WTH*13] WU H.-Y., TAKAHASHI S., HIRONO D., ARIKAWA M., LIN C.-C., YEN H.-C.: Spatially efficient design of annotated metro maps. *Computer Graphics Forum 32*, 3pt3 (2013), 261–270. 2, 3, 4

[WTLY12] WU H.-Y., TAKAHASHI S., LIN C.-C., YEN H.-C.: Travel-route-centered metro map layout and annotation. *Comp. Graph. Forum 31*, 3pt1 (June 2012), 925–934. 3